

## Performance analysis of zone 3 relay with state diagram under transient condition

Kanok Suwannakarn<sup>1\*</sup> and Naebboon Hoonchareon<sup>2</sup>

Department of Electrical Engineering, Chulalongkorn University, Bangkok, Thailand

<sup>1</sup>E-mail: s.kanok@gmail.com

<sup>2</sup>E-mail: naebboon.h@eng.chula.ac.th

\*Corresponding author

Submitted 24 November 2012; accepted in final form 2 May 2013

### Abstract

Operation of a zone 3 distance relay can adversely affect the power system stability in certain severe conditions. An enhanced algorithm of a zone 3 distance relay employing the state diagram is a promising solution that could avoid false operation of such relay. Nonetheless, verification of its performance in transmission test systems under various disturbed conditions is necessary prior to actual implementation. In this study, critical functions of the enhanced zone 3 relay has been examined using the modified 9-bus WSCC test system, with the inclusion of the dynamics of the synchronous generators and the associated excitation and governor controls, which could have significant impacts on the measured voltages under transient periods. Simulated test results have confirmed the effectiveness of the enhanced zone 3 distance relay to differentiate the condition of the system overload from that of the short-circuit fault, and hence, the relay can determine trip signal correctly. However, when the system has encountered the overload condition, immediately followed by the short-circuit fault, it is found that the relay has possibility to miscalculate the situation, and hence, may not send out the trip signal in case the primary protection fails to operate. The role of remote back-up protection that is compromised in such case could still lead to the system blackout, eventually.

**Keywords:** *blackout, zone 3 distance relay, transmission line protection*

### บทคัดย่อ

การทำงานของรีเลย์ระยะทางโซน 3 อาจส่งผลกระทบต่อเสถียรภาพของระบบไฟฟ้ากำลังในบางภาวะวิกฤต การปรับปรุงขั้นตอนวิธีของรีเลย์ระยะทางโซน 3 โดยประยุกต์แผนภูมิสถานะเป็นแนวทางแก้ปัญหามีความเป็นไปได้สูงที่จะช่วยลดโอกาสการทำงานผิดพลาดของรีเลย์ดังกล่าว อย่างไรก็ตาม ก่อนที่จะนำไปใช้งานจริง จำเป็นจะต้องทดสอบสมรรถนะของรีเลย์ป้องกันกับระบบส่งไฟฟ้าจำลองภายใต้เงื่อนไขการรบกวนที่หลากหลาย งานวิจัยนี้ศึกษาวิเคราะห์ฟังก์ชันการทำงานที่สำคัญของรีเลย์ที่ได้รับการปรับปรุงขั้นตอนวิธีดังกล่าว โดยใช้ระบบทดสอบปรับจากระบบ WSCC ที่มีจำนวนบัสไฟฟ้า 9 บัส การจำลองแบบผนวกรวมพลวัตของเครื่องกำเนิดไฟฟ้าเชิงโรตอร์พร้อมทั้งการควบคุมที่เกี่ยวข้องทั้งในระบบกระตุ้นและการควบคุมความเร็วโรเตอร์ซึ่งอาจมีผลอย่างมีนัยยะสำคัญต่อขนาดแรงดันที่รีเลย์ตรวจวัดได้ในภาวะชั่วคราว ผลการศึกษาขึ้นชั้นประสิทธิภาพของรีเลย์ที่ได้รับการปรับปรุงสมรรถนะสามารถจำแนกความแตกต่างของเงื่อนไขการเกิดภาวะโหลดเกินในระบบออกจากเงื่อนไขการเกิดความคิดพ่วงแบบลัดวงจรได้ ส่งผลให้รีเลย์ส่งสัญญาณลัดวงจรได้อย่างถูกต้อง อย่างไรก็ตาม ในกรณีที่เกิดภาวะโหลดเกินขึ้นในระบบแล้วตามมาด้วยความคิดพ่วงแบบลัดวงจรในทันทีนั้น พบว่า รีเลย์ชนิดนี้ยังมีโอกาสประเมินเหตุการณ์ดังกล่าวผิดพลาด และอาจไม่ส่งสัญญาณลัดวงจรในกรณีที่ระบบป้องกันปฐมภูมิไม่ทำงาน ช่องโหว่ของฟังก์ชันการป้องกันแบบสำรองระยะไกลในกรณีดังกล่าวนี้อาจยังคงนำไปสู่เหตุการณ์ไฟฟ้าดับบริเวณกว้างได้ในที่สุด

**คำสำคัญ:** *ไฟฟ้าดับเป็นบริเวณกว้าง, รีเลย์ระยะทางโซน 3, ระบบป้องกันสายส่ง*

### 1. Introduction

Power system stability problems that could lead to system blackout increasingly become a serious concern in operating a complex power system of the present days. One major cause of such severe problems is associated with the existing drawback of the conventional zone 3 distance relay, widely used in a transmission network across the

world. For example, in the US blackout in 2003 (U.S.-Canada Power System Outage Task Force, 2004), the detailed post study revealed that it had been originated by undesirably false trip resulting from the zone 3 distance relay activation, which perpetuated the cascading trips, subsequently. Nevertheless, the zone 3 distance relay remains essential as a remote backup protection for a

transmission line, and therefore, this function could not be abandoned (Horowitz & Phadke, 2006, p.23).

Particularly, the conventional zone 3 relay may misread the condition of system overload to short-circuit fault, in turn, unnecessary trip of at least a few transmission lines may occur. Such false tripping could trigger cascading outages, and result in system blackout, eventually. There were various attempts in the previous works to incorporate some additional rules to the conventional distance relay in order to block the relay from sending a trip signal in the case when overload occurs (Lim, Yuan, Rim, Lee, & Choi, 2006), to prevent the system from the risk of voltage instability (Jonsson & Daalder, 2003). Among those, the proposed zone 3 relay with the addition of a state diagram and a transient index seems quite promising (Kim, Heo, & Aggarwal, 2005) since it is equipped with the mechanism to distinguish the system overload condition from the short-circuit fault, effectively.

This paper aims at verifying performance of the zone 3 relay with the state diagram, on the 9-bus WSCC test system with dynamical effects of the synchronous generators and the associated excitation and governor controls, included. Certain critical transient conditions in a power system have been simulated to determine if the enhanced distance relay can operate, correctly, without compromising the essence of the remote back-up protection for a transmission line. This has been motivated by the previous investigation (Suwannakarn & Hoonchareon, 2007), which found that various conditions of the power system transients could possibly result in trip signal of the relay. The findings in this paper would pave way for actual

implementation of such enhanced relay where it is timely needed for operation of a today's complex power system.

## 2. Objectives

This work intends to examine the discrete performance of the zone 3 state diagram relay (SDR) under some critical transient operating conditions of a power system. The study employs a transmission test system where the dynamics of synchronous generators, excitation systems, and governor controls are also taken into account. There are three main test cases to determine whether the SDR can operate correctly, which are the operations under the short-circuit fault, under the overload condition which is followed by load shedding, and under the overload condition which is followed by short-circuit fault, respectively.

## 3. State diagram relay

The enhanced zone 3 distance relay with state diagram (Kim, Heo, & Aggarwal, 2005), hereafter referred to as State Diagram Relay (SDR), will make a tripping decision based upon state transition of the two input states, which are the Steady-state Component (SC) and the Transient Component (TC), as shown in Figure 1, whereas the conventional distance relay will use only a calculated apparent impedance,  $Z_R$ , to activate a tripping command when  $Z_R$  magnitude encroaches the predefined boundary. In principle, the SDR employs such state transition to distinguish events between the short-circuit fault and the system overload condition, while the conventional distance relay may not have such capability.

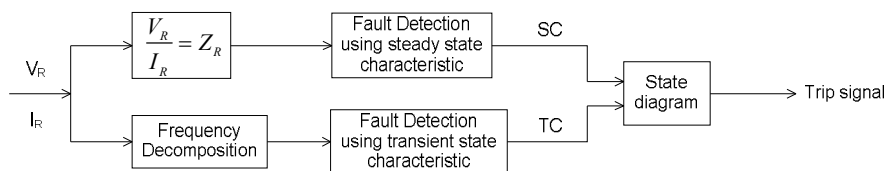


**Figure 1** Process flow of the State Diagram Relay

In Figure 1, the binary state SC is identical to trip signal of the conventional distance relay, whereas the binary state TC is determined relating to transient characteristics of a detected event. In other words, SC will be equal to “1” when the apparent impedance is within zone 3, otherwise it will be

equal to “0”. Additionally, TC can be calculated by comparing the transient index,  $H_{sum}$  as defined below, to the preset threshold relating to transient characteristics of the power system. If  $H_{sum}$  is greater than the threshold, then TC will be set to “1”, else it will be “0”.

$H_{sum}$  can be determined by equations (1) and (2). Firstly, apply Fast Fourier Transform (FFT) to sampled voltage measurements from the voltage transformer of the relay. Then, take the absolute sum of the non-fundamental voltage components to compute for  $H_{sum}$ .

$$V_H(n) = FFT(V) \quad (n = 0, 1, 2, \dots, N-1) \quad (1)$$

$$H_{sum} = \sum_{k=2}^{N/2} |V_H(k)| \quad (2)$$

After that, trip signal will be decided by the state transition diagram of SC-TC, as shown in Figure 2, which is to see whether it will arrive at the Trip state (State 9). Essentially, the 9 plausible states within the state diagram can be grouped into two *Super Zones* – Fault zone on the left, and Load Encroaching zone on the right.

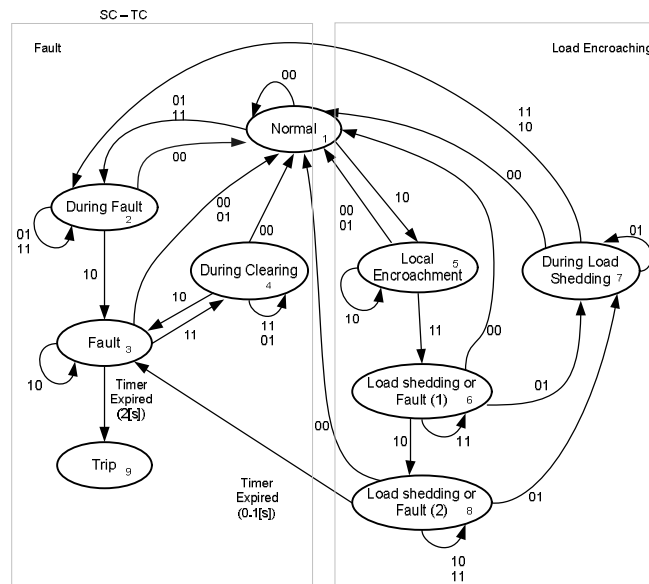


**Figure 2** State diagram for decision making of a trip signal (Kim, Heo, & Aggarwal, 2005, p. 42)

From the proposed scheme, the SDR should generate trip signal only when short-circuit fault occurs, and should not for other incidents, which computationally could also give the state SC equal to 1. Such discrete performance will be examined in the following section, under the three cases of critical transient conditions.

#### 4. Test system and procedures

A single line diagram showing the configuration of the modified 9-bus, WSCC test system (Sauer & Pai, 1998) is shown in Figure 3. The test system is modified by adding parallel circuits for sections 4-5 and 5-7, while also doubling the line lengths to keep the effective impedances the same as those of the original test system. This is to accommodate the tests on operation of a zone 3 distance relay at bus 4, which

has its coverage for the transmission line extended from bus 5 (Horowitz & Phadke, 2006; Anderson, 1999). An SDR, installed at bus 4, is to provide primary protection for line section 4-5, and zone 3 remote back-up protection for line section 5-7, respectively. Operation of other protective relays will be neglected for the purpose of this study.

The system modeled incorporates the dynamics of dq-axis rotor circuits, AVR/PSS excitation systems and speed governors of the three synchronous generators, together with the associated voltage limiters. In addition, all the loads are modeled as a constant power type unless specified otherwise.

Performance analysis of the SDR has been carried out under the three dynamical test cases as described below.

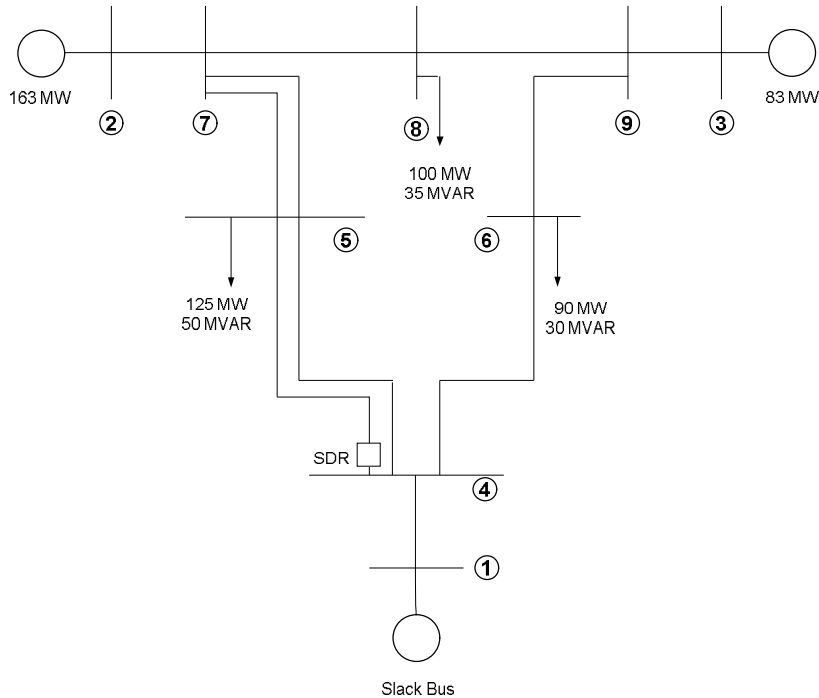


**Figure 3** The modified 9-bus WSCC test system (Sauer & Pai, 1998)

4.1 Testing under short-circuit fault

This experiment is to confirm the remote back-up protection function of the SDR when short-circuit faults do occur. In this case, 3-phase-to-ground fault, with 30-Ω fault resistance, is applied to the middle of one of the parallel lines 5-7. It assumes that zone 1 and zone 2 of all the associated relays fail to operate. Moreover, it also assumes that the fault will be autonomously cleared after 4 seconds with no other transmission lines being removed from the system, for simplicity of the simulation.

4.2 Testing under overload condition followed by load shedding

This experiment is to examine whether the SDR will *NOT* send the trip signal in the case when system overload condition occurs, followed by some load shedding. In this case, real power demand at bus 5 has been continually increased with respect to time until the SDR's sensed apparent impedance encroaches into zone 3, and then, is sustained at that level for another 4 seconds. Following which, if there is no trip command issued by the SDR, then some portion of the increased load will be shed so

that the apparent impedance turns around to outside the zone of protection.

4.3 Testing under overload condition followed by short-circuit fault

This experiment is to examine whether the SDR will *DO* send the trip signal in the case when system overload condition occurs, followed by short-circuit fault. In this case, real power demand at bus 5 has been continually increased with respect to time until the SDR's sensed apparent impedance encroaches into zone 3, and then, is sustained at that level for another 4 seconds. Following which, 3-phase-to-ground fault, with 200-Ω fault resistance, will be applied to one of the parallel lines 5-7, at 80% of the line length distant from bus 5.

To preserve stability of the power system in case 3 so that the system will not be prematurely unstable due to other relevant causes, it assumes that circuit breaker at bus 7 of the faulted line 5-7 will trip instantly after the fault occurs, while that of the non-faulted line 5-7 will trip after 2-second delay, for simulating zone 3 operation. Additionally, the loads at buses 6 and 8 are modeled as a constant

impedance load to support the power system with some helpful damping.

**5. Test results**

Given that the apparent impedance,  $Z_R$  seen by the SDR is equal to  $2.96 + 1.91i$  p.u., at an initial base load, the simulated test results in each respective cases are explained below.

**5.1 Testing under short-circuit fault**

When the fault occurs at the middle of one of the parallel lines 5-7 at time  $t=12$  second, the

locus of apparent impedance seen by the relay at bus 4 is shown in Figure 4. The magnitude of the apparent impedance instantly encroaches into zone 3, and hence, the state SC is triggered to 1. Figure 5 shows the corresponding transients of momentary voltage dip at bus 4, as seen by the relay, during fault period. The voltage signal has dropped to 0.7 p.u. immediately when the fault occurs, and has slightly risen after the protected line 4-5 has been tripped off (by the activation of zone 3 SDR), while the fault still sustains until  $t=16$  second. After that, the voltage is recovered to the nominal value.

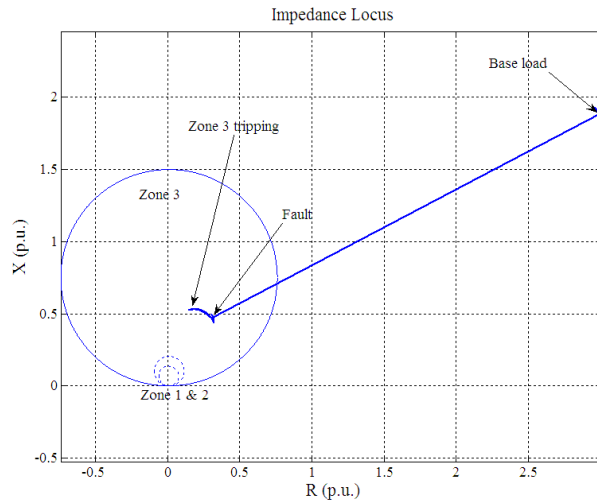


**Figure 4** Apparent impedance locus under short-circuit fault

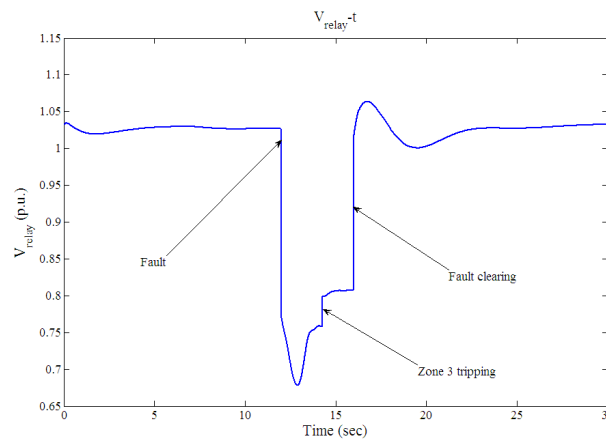


**Figure 5** Voltage sensed by SDR under short-circuit fault

Then, the transient index,  $H_{sum}$ , can be calculated as shown in Figure 6, where the threshold is set to be equal to 25, in this case. By converting the values of  $Z_R$  and  $H_{sum}$  to the corresponding binary states, SC and TC, the sequence of state transition of the SDR can be processed as shown in Figure 7. The

state of SDR has moved from *normal* state 1, to *during fault* state 2, then to *fault* state 3, successively. After the SDR has been trapped at state 3 for longer than 2 seconds, the trip signal is generated, successfully, and the SDR shall return to normal state 1 after that.

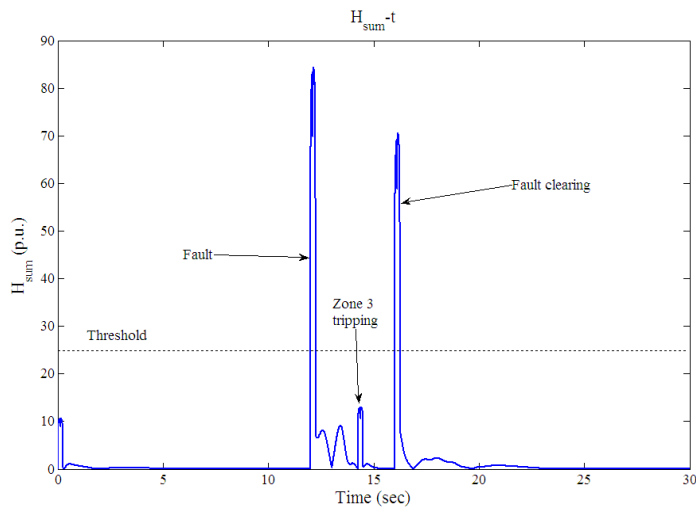


Figure 6 Calculated  $H_{sum}$  under short-circuit fault

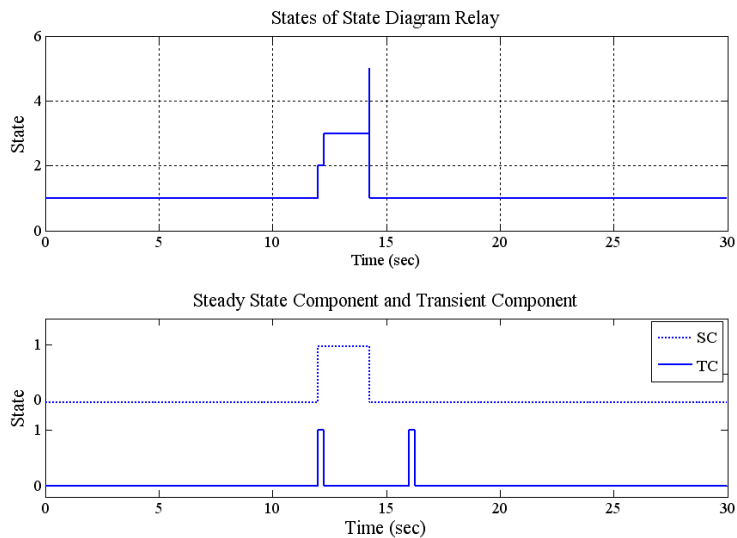


Figure 7 State transition of SDR under short-circuit fault

5.2 Testing under overload condition followed by load shedding

When the system overload condition occurs, followed by some load shedding as described in

section 4, the corresponding test results are shown in Figures 8-11, respectively.

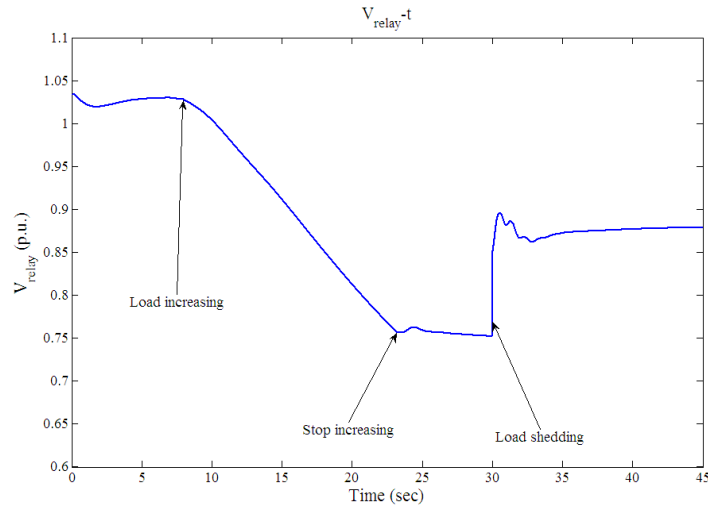


Figure 8 Voltage sensed by SDR under overload condition followed by load shedding

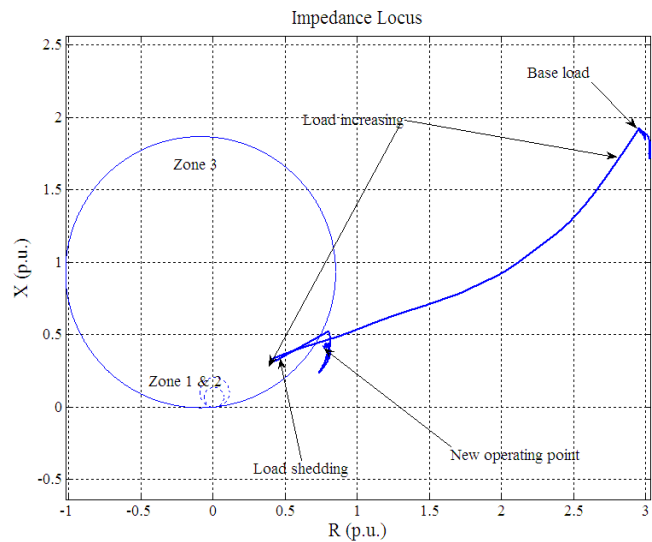


Figure 9 Apparent impedance locus under overload condition followed by load shedding

When load at bus 5 increases, the continued voltage drop sensed by the relay will cause the apparent impedance locus to slowly encroach into zone 3, as shown in Figures 8 and 9. Relatively slow change in voltage response will also keep the transient index,  $H_{sum}$ , close to zero for almost the

entire interval, as in Figure 10. When the load has stopped increasing, then, followed by sudden load shedding by half, the voltage rapidly recovers and the computed  $H_{sum}$  momentarily jumps across the threshold, even though the value is not as high as that in the case of short-circuit fault.

In this case, the sequence of state transition of the SDR, as shown in Figure 11, has been from *normal state 1*, to *local encroachment state 5*, then, return to state 1 after half of the load at bus 5 has been shed. Therefore, the SDR operates correctly as

it will not send a trip signal, whereas the conventional zone 3 relay would do so since the detected apparent impedance has been in zone 3 longer than the 2-second time delay.

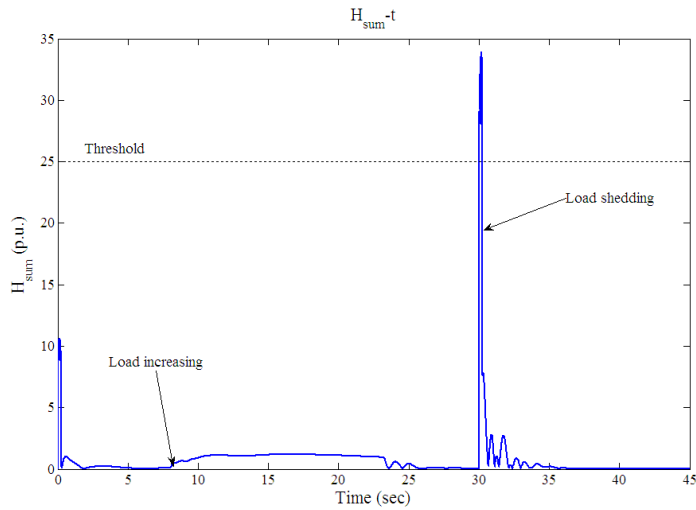


Figure 10 Calculated  $H_{sum}$  under overload condition followed by load shedding

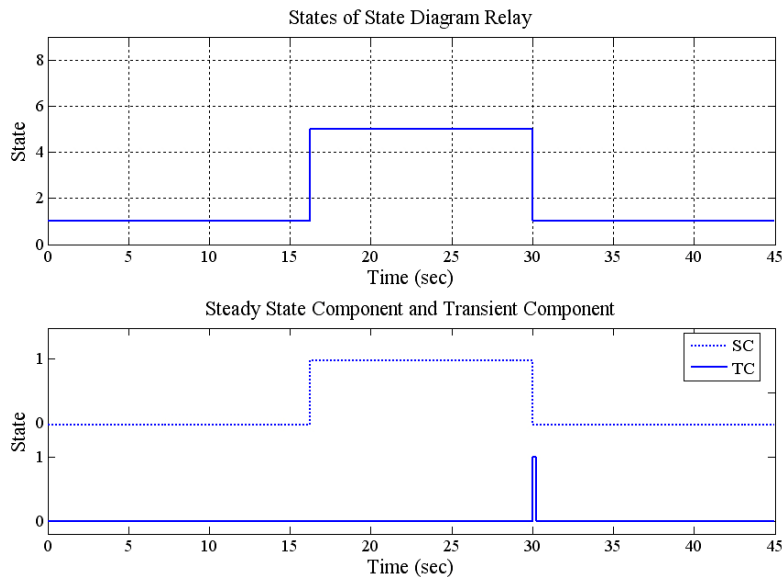


Figure 11 State transition of SDR under overload condition followed by load shedding

5.3 Testing under overload condition followed by short-circuit fault

When the system overload condition occurs, followed by the 3-phase-to-ground fault, with 200-Ω fault resistance, on one of the parallel lines 5-7, as described in section 4, the corresponding test results

are shown in Figures 12-15, respectively. Additionally, dynamical behaviors of the generator terminal voltages of the three generating units are also presented in Figures 16 and 17, comparing between the cases when the SDRs do, and do not, send the trip signals.

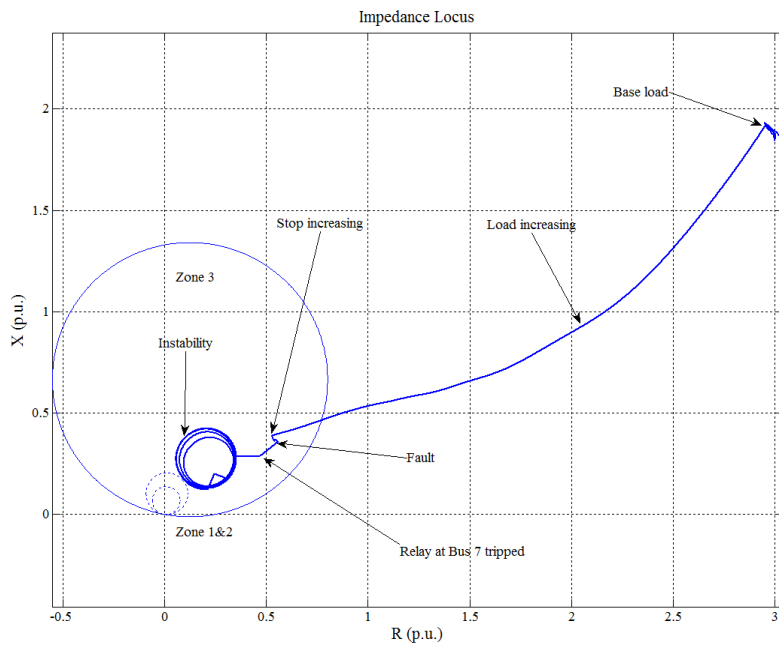


Figure 12 Apparent impedance locus under overload condition followed by short-circuit fault

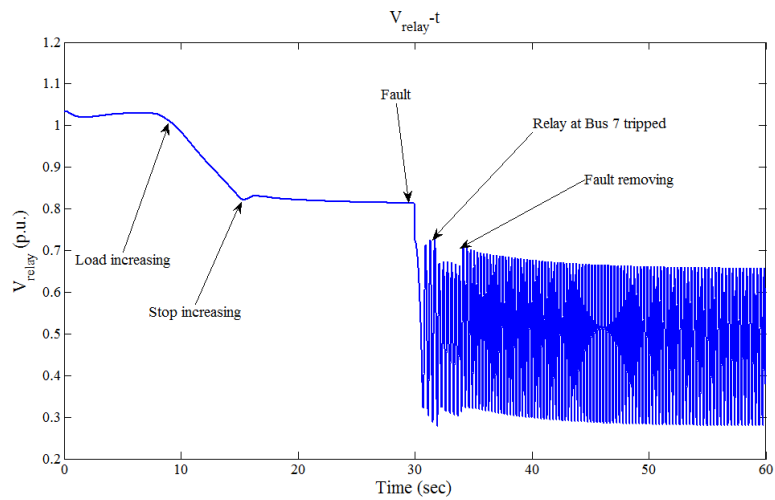


Figure 13 Voltage sensed by SDR when overload occurs, followed by short-circuit fault

Obviously, during time interval 0-30 seconds, the test results obtained have been the same as those respective results in case 2. Then, when the fault occurs at  $t=30$  second, and it assumes that the faulted line and non-faulted line 5-7 are tripped as described in section 4 while the fault currents are still being fetched from other directions, the apparent impedance will sustain even longer within zone 3 with decreasing magnitude. Meanwhile, the value of  $H_{sum}$  will rapidly increase above the threshold, caused by the large disturbance of fault.

Consequently, Figure 15 reveals that the state transition of the SDR will move from *local encroachment* state 5, at time  $t=30$  second, to states

$\rightarrow 6 \rightarrow 8 \rightarrow 3$ , respectively, which seems to be in the right direction. However, due to the assumption that the associated primary protection fails to completely clear the fault, power system oscillation associated with the short-circuit fault, which can also be observed from the voltage measurements, will concurrently keep the value of  $H_{sum}$  fluctuating across, and mostly above the threshold. In turn, the state of the SDR will be trapped either in the *fault* state 3, or *during clearing* state 4, with no trip signal being sent out to the circuit breaker, until the entire power system goes unstable due to loss of synchronism among the three generators, as clearly seen in Figures 13 and 16.

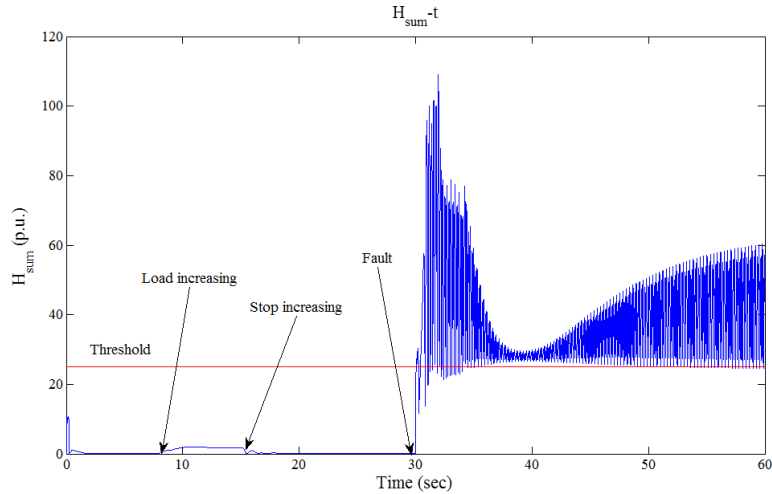


Figure 14 Calculated  $H_{sum}$  under overload condition followed by short-circuit fault

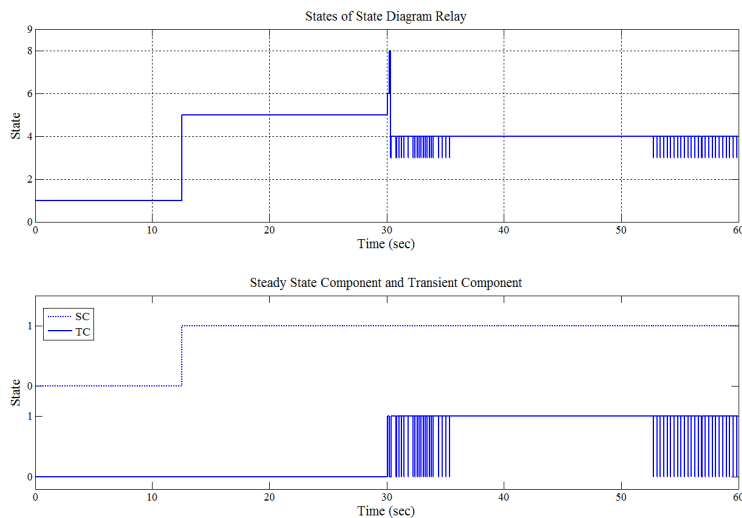
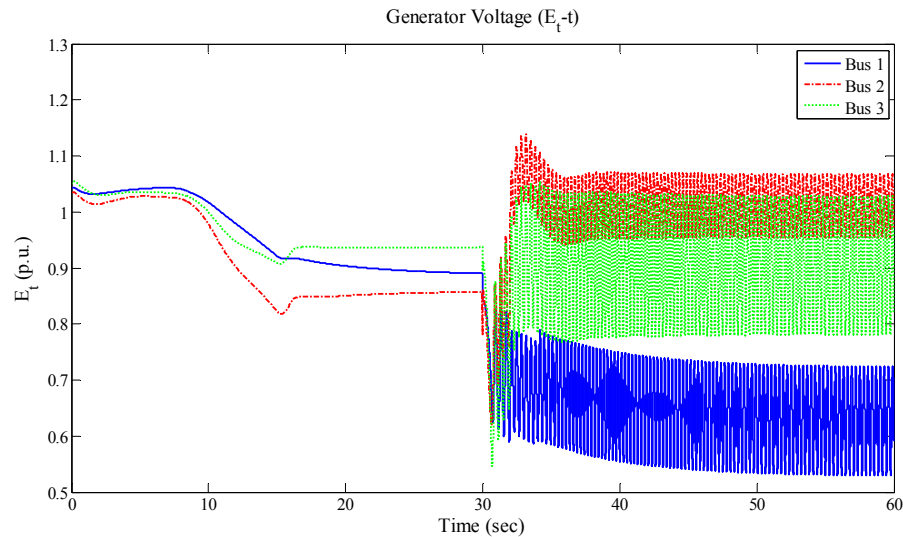


Figure 15 State transition of SDR under overload condition followed by short-circuit fault



**Figure 16** Dynamical behaviors of the generator terminal voltages when SDR no trip (Unstable)

## 6. Discussion

Simulated test results in case 1 and case 2 support the findings in the previous work (Kim, Heo, & Aggarwal, 2005), when verifying on a test system with more detailed dynamics of a power generation and transmission included, that the SDR can provide remote back-up protection to transmission lines similar to the conventional zone 3 distance relay can do when the short-circuit fault occurs. Moreover, the SDR can prevent undesirable line tripping due to the system overload condition, as well as the associated load shedding that may follow, even though the detected apparent impedance falls into zone 3 sufficiently long. Such undesirable line tripping could accelerate voltage instability problem, and lead to system blackout. To attain such enhanced performance, the binary variable TC plays a crucial role in distinguishing those two classes of events.

Case 3 is intended to investigate the aspect of priority assigned to the short-circuit protection, which should supersede that assigned to the load encroachment trip blocking. The previous work of reference (Kim, Heo, & Aggarwal, 2005) demonstrated that the SDR could correctly operate in a complicated situation where three-phase fault

occurs during heavy loading condition. Nonetheless, due to limitation of the model used for the study, it has not yet taken into account the effects of power system oscillation which could be directly associated with the short-circuit faults.

In case 3, it can be implied from the test results that the SDR could detect the fault existence, but could not determine whether the fault has already been cleared (by other higher-priority zone 1, or zone 2 relays in coordination). Hence, the sustained fault which could not be isolated in due time brings about loss of synchronism, eventually.

Finally, for demonstration purpose pertinent to the test results in case 3, should the SDR have sent the trip command to the circuit breaker after 2-second time delay, and therefore, the fault would have been completely isolated from the rest system, it was found that stability of the rest power system could be well preserved after a few seconds of power oscillation experienced, as illustrated in Figure 17, below. All three generator terminal voltages could have returned to nominal value after the faulted part, including the heavy load at bus 5, had been removed. Hence, the system blackout could have been avoided, in such case.

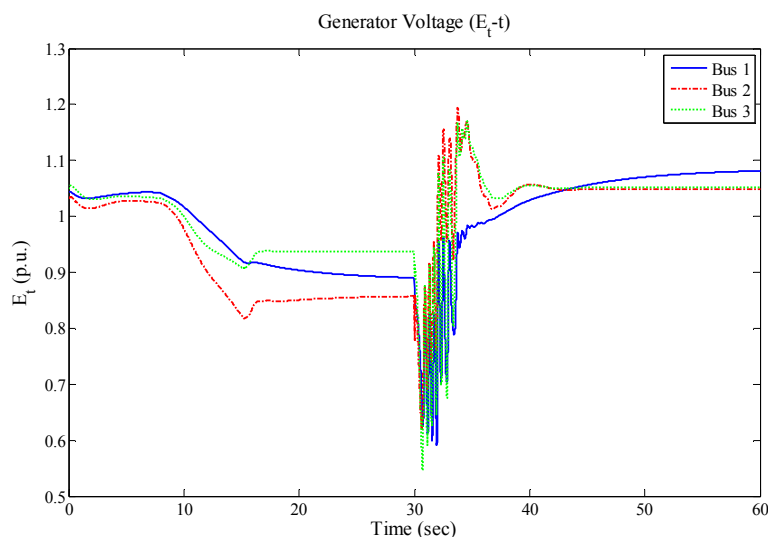


Figure 17 Dynamical behaviors of the generator terminal voltages when SDR trips (Stable)

## 7. Conclusion

This paper verifies performance of the enhanced zone 3 relay with state diagram under certain critical transient conditions, which are short-circuit fault, overload condition followed by load shedding, and overload condition followed by short-circuit fault, respectively. Test results obtained when testing on the 9-bus, WSCC transmission test system with the inclusion of the dynamics of the synchronous generators and the associated excitation and governor controls, confirm that the enhanced state diagram relay can effectively differentiate the condition of the system overload from that of the short-circuit fault, and hence, can operate correctly without compromising the essence of the remote back-up protection. Nonetheless, when the system has encountered overload condition, immediately followed by the short-circuit fault, it is found that the state diagram relay may not send out the trip command in case the primary protection fails to operate, primarily due to signal contamination as a result of power oscillation. The role of back-up protection that is compromised in such case could lead to the system blackout, eventually. Further improvement of the state diagram relay to address this plausible loophole would strongly encourage actual implementation of such enhanced relay where it is much needed for operation of a complex power system of the present days.

## 8. Acknowledgement

Funding support from “Chulalongkorn University Graduate Scholarship to Commemorate The 72<sup>nd</sup> Anniversary of His Majesty King Bhumibol Adulyadej” has been gratefully acknowledged.

## 9. References

- Anderson, P. M. (1999). *Power System Protection*. New York, US: IEEE PRESS and McGraw-Hill, Inc.
- Horowitz, S. H., & Phadke, A. G. (2006). Third zone revisited. *IEEE Transactions on Power Delivery*, 20(1), 23-29.
- Jonsson, M., & Daalder, J. (2003). An adaptive scheme to prevent undesirable distance protection operation during voltage instability. *IEEE Transactions on Power Delivery*, 18(4), 1174-1180.
- Kim, C. H., Heo, J. Y., & Aggarwal, R. K. (2005). An enhanced zone 3 algorithm of a distance relay using transient components and state diagram. *IEEE Transactions on Power Delivery*, 20(1), 39-46.
- Lim, S. I., Yuan, H. C., Rim, S. J., Lee, S. J., & Choi, M. S. (2006). Adaptive blinder for distance relay based on sensitivity factors. *International Conference on Power System Technology*, 1(1), 1-5.

- Sauer, P. W., & Pai, M. A. (1998). *Power System Dynamics and Stability*. New Jersey, US: Prentice Hall.
- Suwannakarn. K., & Hoonchareon, N. (2007). Performance analysis of the zone 3 distance relay with state diagram under dynamics and control of the synchronous generator. *EECON-30*, 313-316.
- U.S.-Canada Power System Outage Task Force. (2004). *Final Report on the August 14, 2003 Blackout in the United States and Canada: Causes and Recommendations*. Retrieved from <http://www.ferc.gov>